Effective Coulomb interactions within BEDT-TTF dimers

Edan Scriven* and B. J. Powell
Centre for Organic Photonics and Electronics, School of Mathematics and Physics, University of Queensland, Queensland 4072, Australia

(Received 28 July 2009; revised manuscript received 1 October 2009; published 6 November 2009)

We calculate the parameters for Hubbard models of κ-(BEDT-TTF)$_2X$ and β-(BEDT-TTF)$_2X$. We use density-functional theory (DFT) to calculate the interactions between holes in dimers of the organic molecule bis(ethylenedithio)tetrathiafulvalene (BEDT-TTF) for 23 experimental geometries taken from a range of materials in both the β and κ polymorphs. We find that the effective Coulomb interactions are essentially the same for all of the compounds studied. We highlight the disagreement between our parametrization of the Hubbard model and previous results from both DFT and Hückel methods. We show that this is caused by the failure of an assumption made in previous calculations (which estimate the effective Coulomb interaction from the intradimer hopping integral). We discuss the implications of our calculations for theories of the BEDT-TTF salts based on the Hubbard model and use our calculated parameters to explain a number of phenomena caused by conformational disorder in these materials.

DOI: 10.1103/PhysRevB.80.205107 PACS number(s): 71.27.+a, 74.70.Kn, 71.10.Fd

I. INTRODUCTION

One of the most pressing problems in condensed-matter physics is to understand and control phenomena that result from strong electronic correlations.[1] A major bottleneck in this task is that first-principles calculations often do not provide a quantitatively (or, in many systems, qualitatively) correct description of strongly correlated electrons.[2] This means that strongly correlated materials are often studied on the basis of simple models whose parameters are not known. Clearly this impedes direct comparison with experiment.

Organic materials present an inviting playground to explore strong electronic correlations because of the inherent flexibility and control of organic chemistry. This allows one to study stoichiometric (and hence clean) materials with relatively low absolute energy scales such as the organic charge-transfer salts. This has a number of advantages both in terms of carrying out a wide range of experiments and, potentially, for constructing a microscopic theory from first principles.

While there has been recent progress in combining density-functional theory (DFT) with more advanced numerical techniques,[3] another promising approach is to use electronic-structure calculations to parameterize effective low-energy Hamiltonians, which can then be studied by any number of analytical or numerical methods.[4] Here we take the latter approach.

Layered organic charge-transfer salts of the form (ET)$_2X$, where ET is bis(ethylenedithio)tetrathiafulvalene or BEDT-TTF and X is a monovalent anion, exhibit a variety of unusual phenomena due to the strong electronic correlations present in these materials.[5] These phenomena include unconventional superconductivity[5] with a small superfluid stiffness,[6] a Mott insulator,[7] a spin liquid,[8] strongly correlated[9,10] and unconventional[10,11] metallic states, and a pseudogap.[12] Experimentally, one can tune between these phases by varying the temperature and pressure (including both hydrostatic and "chemical" pressure, i.e., varying the anion, X).[5]

DFT band-structure calculations of ET crystals,[13–15] find a half-filled valence band and hence a metallic state. However, these calculations do not recover the Mott insulating state or the other strongly correlated effects that are observed experimentally. Therefore, efforts have focused on the application of effective low-energy Hamiltonians such as Hubbard models.[5] However, in molecular crystals, the effective parameters for such low-energy Hamiltonians may be calculated from studying the properties of single molecules or small molecular clusters, which may be accurately described by DFT.[4,16–21]

ET salts occur in a variety of crystal packing structures. In the β and κ polymorphs the ET molecules form dimers. Intradimer dynamics are often integrated out of effective low-energy models of β-(ET)$_2X$ and κ-(ET)$_2X$. In these charge-transfer salts, each dimer donates one electron to the anion layers to form a half-filled system. Both Hückel[22] and DFT (Refs. 13–15) calculations have found that the dimers form an anisotropic triangular lattice in which each lattice site is a dimer. However, there is a strong effective Coulomb repulsion, U_d, between two electrons on the same dimer, which must be included in the effective low-energy description.[5,23] The electronic interactions within an ET dimer are stronger than those between an ET molecule and its next-nearest neighbors on the crystal lattice. Therefore, these materials have been widely studied on the basis of Hubbard models.[5] In order to explain the observed physics these theories assume that both chemical and hydrostatic pressures reduce U_d/W, where W is the bandwidth. Therefore, an important task for the field is to understand how this ratio varies with chemical and hydrostatic pressures.

Previously, the on-site Coulomb repulsion term in the Hubbard model, U_d, has been estimated from both Hückel[24–31] and density-functional[14,15] calculations under the assumptions that the intramonomer Coulomb repulsion $U_m \rightarrow \infty$, and the intermonomer Coulomb repulsion $V_m \rightarrow 0$. We will show below that this assumption is incorrect and leads to a systematic underestimate of U_d.

Disorder plays a number of important roles in organic superconductors.[32] Increasing the degree of disorder leads to a suppression of the superconducting critical temperature, T_c, which is correlated with a rise in the residual resistivity.[32] Further disorder, via impurity-assisted tunnelling in the interlayer direction, can lead to violations of Matthiessen's rule[33]

and an additional incoherent channel in magnetoresistance experiments.[34]

In κ-$(ET)_2Cu[N(CN)_2]Br$ the degree of disorder can be increased by increasing the rate at which the sample is cooled,[35–39] which leads to a suppression of T_c by ~ 1 K. Further, increasing the cooling rate can drive the system toward the insulating side of the metal-insulator transition.[38] Two hypothesis have been proposed for the source of this disorder: terminal ethylene-group disorder[35–38] and disorder in the anion layer.[40] Therefore it is important to estimate the scattering rate caused by terminal ethylene disorder in this material.

Even more dramatic effects are observed in β-$(ET)_2I_3$. Variations in the pressure as the sample is cooled can change the ambient pressure T_c from 1 (for samples cooled at ambient pressure; known as the β_L phase) to 7 K (for samples cooled at $P \gtrsim 1$ kbar once the pressure is released; known as the β_H phase).[41] In this material clear differences in the terminal ethylene groups in the β_H and β_L phases are observed via x-ray scattering.[42] Thus it has been argued that the terminal ethylene disorder is responsible for the differences in the critical temperatures between the β_H and β_L phases.[43]

In order to study the role of impurity scattering caused by conformational disorder in the terminal ethylene groups of the ET molecule in the phenomena discussed above, we also present calculations of the effective site energy for holes in the β- and κ-phase salts.

In this paper we present DFT calculations for ET dimers in vacuum. In Sec. II we describe the computational method by which we calculate these energies. In Sec. III we discuss the problem for the isolated dimer and review the parametrization of the two-site extended Hubbard model from the total energies of the relevant $(ET)_2$ charge states. In Sec. IV we report and discuss the resulting values of the Hubbard parameters. In Sec. V we draw our conclusions.

II. COMPUTATIONAL METHODS

We used DFT to calculate the total energies of ET dimers in various conformations and charge states. We used the SIESTA (Ref. 44) implementation of DFT, with the exchange-correlation functional of Perdew, Burke, and Ernzerhof,[45] a triple-ζ plus single polarization (TZP) basis set (except where we explicitly specify otherwise) and basis functions consisting of Sankey-type numerical atomic orbitals.[46] The orbital functions were confined to a radius r_c from their centers, which slightly increases the energy of the orbital. The specified maximum allowed increase in energy due to this cutoff was 2 mRy. The convergence of the integration mesh was determined by specifying an effective plane-wave cutoff energy of 250 Ry. The initial spin moments on each atom were arranged antiferromagnetically wherever possible. We used pseudopotentials constructed according to the improved Troullier-Martins (TM2) method.[47]

Nuclear positions for C and S atoms were obtained from x-ray crystallography.[24,25,48–53] H atoms, which are not observed in x-ray scattering experiments, were relaxed by the conjugate-gradient method. Total DFT energy differences between the relevant charge states $[E(1)-E(0)]$ and $[E(2)-E(0)]$ were equated with the corresponding analytical expressions in Eq. (5) to determine the Hubbard parameters. We focus on these "experimental" geometries rather than performing a full relaxation for a number of reasons. First, there are small differences in the reported geometries for different ET salts and one would like to understand the effect of these. Second, the experiments effectively "integrate over" all of the relevant charge states and therefore provide an "average" conformation. Third, the experiments naturally include the effects on the molecular conformation due to the crystalline environment, which are absent from *in vacuo* calculations.

III. TWO-SITE EXTENDED HUBBARD MODEL

In calculations of the effective Coulomb interaction (the Hubbard U) in molecular solids it is important to recognize that their are two contributions.[4,16–21] That is, the effective Coulomb interaction on a ET dimer may be written as

$$U_d = U_d^{(v)} - \delta U_d^{(p)}, \tag{1}$$

where $U_d^{(v)}$ is the value of U_d for the dimer cluster in vacuum and $\delta U_d^{(p)}$ is the reduction in U_d from the polarizable crystalline environment. Calculating $\delta U_d^{(p)}$ for ET salts is a highly nontrivial problem due to the large size of the ET molecule relative to the intermolecular spacing. Below we present results of DFT calculations for $U_d^{(v)}$ of dimers in the conformations found in a wide range of κ- and β-phase ET salts. Similar results hold for U_m, the effective Coulomb repulsion between two holes on the same monomer and V_m the effective Coulomb interaction between two holes on neighboring monomers. Below we will primarily discuss the vacuum contributions to these terms, $U_m^{(v)}$ and $V_m^{(v)}$.

The effective vacuum intradimer Coulomb energy, $U_d^{(v)}$, is given by (see, e.g., Ref. 16)

$$U_d^{(v)} = E(0) + E(2) - 2E(1), \tag{2}$$

where $E(q)$ is the ground-state energy of the dimer in vacuum containing q holes, i.e., with charge $+q$. Similarly, the effective site energy for holes is given by

$$\xi_d = E(0) - E(1). \tag{3}$$

Below we calculate $E(q)$ via density-functional methods.

It is also interesting to consider intradimer dynamics, which can be described via a two-site extended Hubbard model,[5]

$$\hat{\mathcal{H}} = \sum_{i\sigma} \xi_{mi} \hat{n}_{i\sigma} - t \sum_{\sigma} (\hat{h}_{1\sigma}^{\dagger} \hat{h}_{2\sigma} + \text{H.c.}) + \sum_{i} U_{mi} \hat{n}_{i\uparrow} \hat{n}_{i\downarrow} + V_m \hat{n}_1 \hat{n}_2, \tag{4}$$

where $\hat{h}_{i\sigma}^{(\dagger)}$ annihilates (creates) a hole on site (monomer) i in spin state σ, ξ_{mi} is the site energy for holes on site i, $\hat{n}_{i\sigma}$ is the number operator for spin σ holes on site i, $\hat{n}_i = \Sigma_\sigma \hat{n}_{i\sigma}$, t is the intradimer hopping integral, U_{mi} is the effective on-site (monomer) Coulomb repulsion, and V_m is the intersite Coulomb repulsion (Fig. 1).

The lowest-energy eigenvalues of Hamiltonian (4) for each charge state are

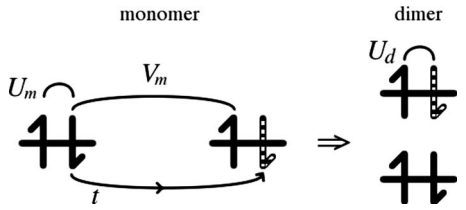

FIG. 1. Schematic of the Hubbard models studied in this paper. The left panel shows the two-site extended Hubbard model. Here each site represents a monomer (single ET molecule). The Coulomb interactions (U_m between electrons on the same monomer and V_m between electrons on different monomers) and the hopping integral, t, are marked. The right panel shows the dimerized model. As the bonding orbital is filled only a single state is relevant, thus the only parameter is the effective Coulomb repulsion between electrons/holes in that state, U_d.

$$E(0) = 0, \tag{5a}$$

$$E(1) = \bar{\xi}_m - \frac{1}{2}\sqrt{4t^2 + (\Delta\xi_m)^2}, \tag{5b}$$

$$E(2) = 2\bar{\xi}_m + \frac{1}{3}(2\bar{U}_m + V_m - 2A\cos\theta), \tag{5c}$$

where $\bar{\xi}_m = \frac{1}{2}(\xi_{m1} + \xi_{m2})$, $A = 12t^2 + (\Delta U_m)^2 + (U_{m1} - V_m)(U_{m2} - V_m) + 3(\Delta\xi_m)^2$, $\cos 3\theta = (\bar{U}_m - 2V_m)[18t^2 - (2U_{m1} - U_{m2} - V_m) \times (U_{m1} - 2U_{m2} + V_m) - 9(\Delta\xi_m)^2]/2A^3$, $\Delta\xi_m = \xi_{m1} - \xi_{m2}$, $\bar{U}_m = \frac{1}{2}(U_{m1} + U_{m2})$, and $\Delta U_m = U_{m1} - U_{m2}$.

We have previously calculated ξ_m and $U_m^{(v)}$ from the one-site Hubbard model for an ET monomer for the experimentally observed conformations in all the materials discussed below,[16] therefore one may solve Eqs. (5) for t and V_m taking ξ_m and $U_m^{(v)}$ from the monomer calculations. The case of two monomers with different site energies and on-site Coulomb repulsion may be solved by a general method for diagonalizing cubic matrix eigensystems.[54] In cases where the two monomers within a dimer have the same geometry (e.g., by symmetry), $\xi_{m1} = \xi_{m2} = \xi_m$ and $U_{m1} = U_{m2} = U_m$ and the eigenvalues simplify to

$$E(1) = \xi_m - t, \tag{6a}$$

$$E(2) = 2\xi_m + \frac{1}{2}(U_m + V_m - \sqrt{16t^2 + (U_m - V_m)^2}), \tag{6b}$$

in which case the solution is straightforward.

In the limit $U_m = V_m = 0$ the two-site Hubbard model has two solutions: the bonding state $|\phi_{b\sigma}\rangle = |\phi_{1\sigma}\rangle + |\phi_{2\sigma}\rangle$ and the antibonding state $|\phi_{a\sigma}\rangle = |\phi_{1\sigma}\rangle - |\phi_{2\sigma}\rangle$, where $|\phi_{i\sigma}\rangle = \hat{h}_{i\sigma}|0\rangle$ is a single-electron state centered on the ith monomer and $|0\rangle$ is the (particle) vacuum state.

In Figs. 2 and 3 we plot the highest-occupied molecular orbitals (HOMOs) of ET dimer for the conformations found in β-$(ET)_2I_3$ and κ-$(ET)_2Cu_2(CN)_3$, respectively, in both the charge neutral and the 2+ states. It can be seen that these dimer orbitals are the antibonding and bonding hybrids of the ET monomer HOMO (shown in Fig. 4), respectively. The most important difference between the orbital geometries lies in the S···S intermonomer contacts, which contain nodes in the antibonding orbital but are connected in the bonding or-

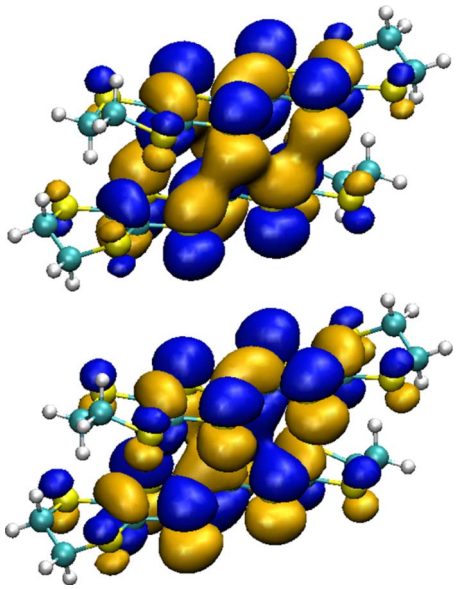

FIG. 2. (Color online) The HOMO of $(ET)_2^{2+}$ (top) and charge neutral $(ET)_2$ (bottom), with nuclear positions from the crystal β-$(ET)_2I_3$. The HOMO of $(ET)_2^{2+}$ is the dimer bonding orbital and the HOMO of $(ET)_2$ is the antibonding orbital of the two ET HOMOs (cf. Fig. 4). The essential difference between the two lies in the relative phase of the orbital function on each molecule. The bonding orbital connects the ET molecules at the S···S contacts (cf. Fig. 8). In the antibonding orbital, there are nodes between the S···S contacts.

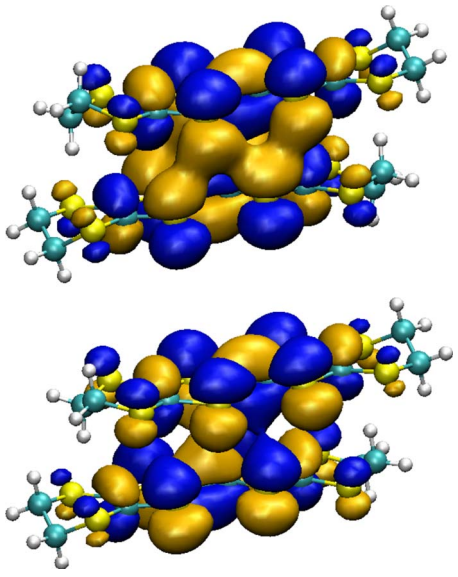

FIG. 3. (Color online) The HOMO of $(ET)_2^{2+}$ (top) and charge neutral $(ET)_2$ (bottom), with nuclear positions from the crystal κ-$(ET)_2Cu_2(CN)_3$. The similarity of the nuclear structures and orbitals between this conformation and the β conformation in Fig. 2 highlight the dimer as a common structural unit within two different packing motifs.

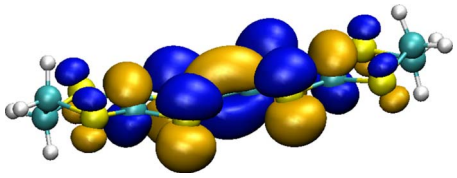

FIG. 4. (Color online) The HOMO of a charge neutral ET monomer, with nuclear positions from the crystal β-$(ET)_2I_3$. This is the orbital from each molecule that contributes to the HOMO of the $(ET)_2$ and $(ET)_2^{2+}$ dimers.

bital. Thus the DFT picture of the $(ET)_2$ system is remarkably similar to the molecular-orbital description of a diatomic molecule[4] but with the "covalent bond" between the two monomers rather than between two atoms.

IV. CALCULATION OF THE HUBBARD-MODEL PARAMETERS

A. Basis-set convergence

We tested the basis-set convergence of the DFT calculations using the conformation observed in κ-$(ET)_2Cu(NCS)_2$ as the test case, with single-ζ (SZ), single-ζ plus polarization (SZP), double-ζ (DZ), double-ζ plus polarization (DZP), and TZP basis sets. We also calculated the monomer parameters, U_m and ξ_m, in each basis, using the method we previously applied to the ET monomers.[16] The Hubbard-model parameters in each basis set are reported in Fig. 5. The values of all parameters are well converged in the TZP basis, except t. t is an order of magnitude smaller than the other parameters, and on the order of both the variation in the other parameters among the basis sets tested and the uncertainty associated with the calculation method. This suggests that extracting t from band-structure calculations[14,15] may be a more reliable method of estimating the hopping integrals in these systems.

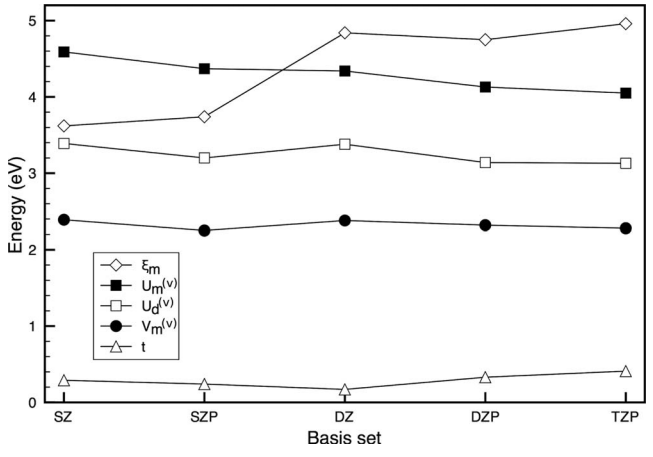

FIG. 5. Variation in Hubbard parameters found from DFT calculations with basis set, which improve from left to right. The test conformation is taken from the crystal κ-$(ET)_2Cu(NCS)_2$ (Ref. 25). All of the quantities except t are well converged at TZP, the basis set chosen for all subsequent calculations. Indeed, ξ_m is the only other quantity that changes significantly across the range of basis sets. However, t is a relatively small quantity, on the order of its own variations with respect to basis-set size. Hence we conclude that solving the Hamiltonian (4) is not an accurate method for finding t.

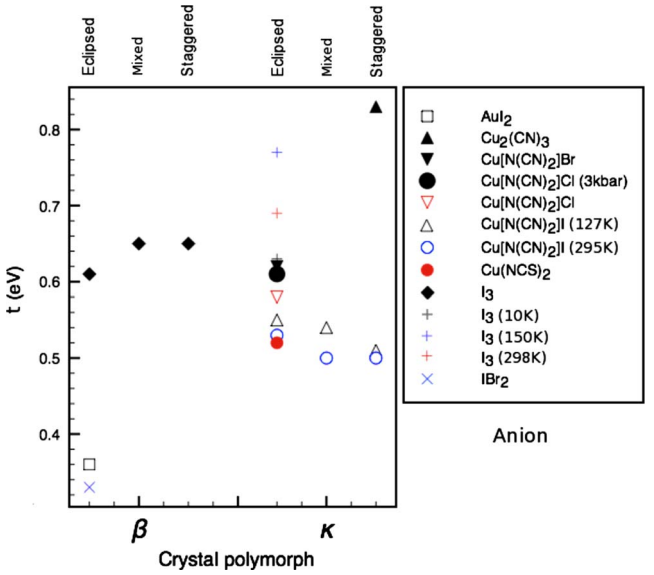

FIG. 6. (Color online) Intermonomer hopping term, t, for various ET dimers. The mean value for β-$(ET)_2X$ crystals is $t=0.54\pm0.15$ eV, although there is an apparent grouping of β-$(ET)_2I_3$ about $t\sim0.64$ eV while the other β crystals have $t\sim0.35$ eV. For κ-$(ET)_2X$ crystals, the value of $t=0.59\pm0.10$ eV. These results suggest that in terms of the delocalization effect of dimerization, either β-$(ET)_2I_3$ more closely resembles the κ-ET crystals than its fellow β crystals or t is essentially the same for both crystal polymorphs and the low value of t for β-$(ET)_2AuI_2$ and β-$(ET)_2IBr_2$ is unusual.

B. Variation in the intradimer hopping integral

The above considerations notwithstanding, we report our intradimer hopping integrals in values in Fig. 6 for the purpose of comparison to previous estimates from DFT and Hückel methods (see Table I). For β-$(ET)_2X$ crystals, $t=0.54\pm0.15$ eV. For κ-$(ET)_2X$ crystals, $t=0.59\pm0.10$ eV. These values are at the high end of the range presented in Table I but are, nevertheless, consistent with previous estimates.

C. Variation in the intradimer Coulomb repulsion

Now we consider variation in the effective Coulomb interactions across the conformations found in different materials, beginning with $U_d^{(v)}$. In Fig. 7 we show the values of $U_d^{(v)}$ for the conformations observed experimentally in a variety of ET crystals. Of particular note are the three data points corresponding to different possible conformations of β-$(ET)_2I_3$. In the ET molecule the terminal ethylene groups may take two relative orientations known as the staggered and eclipsed conformations (cf. Fig. 8). $U_d^{(v)}$ is smallest when both ET molecules are in the staggered conformation. Conversely, the largest $U_d^{(v)}$ for this crystal occurs when both ET molecules are eclipsed, with intermediate $U_d^{(v)}$ values for the case with one staggered and one eclipsed ET molecule. This

TABLE I. Previous estimates of $U_d^{(v)}$ for various β- and κ-phase ET salts. These values were obtained from both Hückel and density-functional methods under the assumptions $U_m^{(v)} \to \infty$ and $V_m^{(v)} = 0$, which yields $U_d^{(v)} = 2t$. These estimates substantially underestimate the actual value of $U_d^{(v)}$ (see Fig. 7) as $U_m^{(v)} \sim V_m^{(v)}$. The two-site extended Hubbard model produces values of t on the same order of magnitude as these Hückel calculations. One should also note the wide scatter between the different Hückel calculations, even between different studies of the same material.

Crystal	Method	$U_d^{(v)}$ (eV)
β-$(ET)_2I_3$	Hückel[a]	0.49
β-$(ET)_2IBr_2$	Hückel[b]	0.98
β-$(ET)_2ICl_2$	Hückel[b]	1.04
β-$(ET)_2I_3$	Hückel[a]	0.49
β-$(ET)_2CH(SO_2CF_3)_2$	Hückel[c]	0.88–0.90
β-$(ET)_2[OsNOCl_5]$	Hückel[d]	2.10
κ-$(ET)_2Cu[N(CN)_2]Cl$	DFT[e]	0.4
κ-$(ET)_2Cu[N(CN)_2]Br$	Hückel[f]	0.45
κ-$(ET)_2Cu(NCS)_2$	Hückel[g]	0.48
κ-$(ET)_2Cu(NCS)_2$	Hückel[h]	0.14
κ-$(ET)_2Cu(NCS)_2$	Hückel[i]	0.46
κ-$(ET)_2Cu(NCS)_2$	DFT[j]	0.83
κ-$(ET)_2Cu(NCS)_2$	DFT[e]	0.4
κ-$(ET)_2Cu[N(CN)_2]Br$	Hückel[i]	0.49
κ-$(ET)_2Cu_2(CN)_3$	Hückel[i]	0.45
κ-$(ET)_2Cu_2(CN)_3$	DFT[j]	0.85
κ-$(ET)_2Cu_2(CN)_3$	DFT[e]	0.4
κ-$(ET)_2I_3$	Hückel[i]	0.49
κ-$(ET)_2I_3$	Hückel[k]	0.22

[a]Reference 26.
[b]Reference 27.
[c]Reference 28.
[d]Reference 29.
[e]Reference 15.
[f]Reference 30.
[g]Reference 31.
[h]Reference 25.
[i]Reference 55.
[j]Reference 14.
[k]Reference 24.

trend is repeated in the κ-phase crystals, where two data sets (corresponding to different temperatures at which the nuclear positions were determined) for κ-$(ET)_2Cu[N(CN)_2]I$ provide data for both conformations.

The mean value of $U_d^{(v)}$ for the β-phase crystals is 3.19 ± 0.07 eV and the mean $U_d^{(v)}$ for the κ-phase crystals is 3.23 ± 0.09 eV. The quoted error is one standard deviation over the full set of conformations studied. The difference between the two values of $U_d^{(v)}$ is $\sim 1\%$ and well within the error ranges. This suggests that $U_d^{(v)}$ takes the same value, 3.2 eV, in all β- and κ-phase ET salts. This result is significantly larger than the value of $U_d^{(v)}$ obtained from Hückel calculations ($\sim 0.5-2$ eV), as we will discuss below.

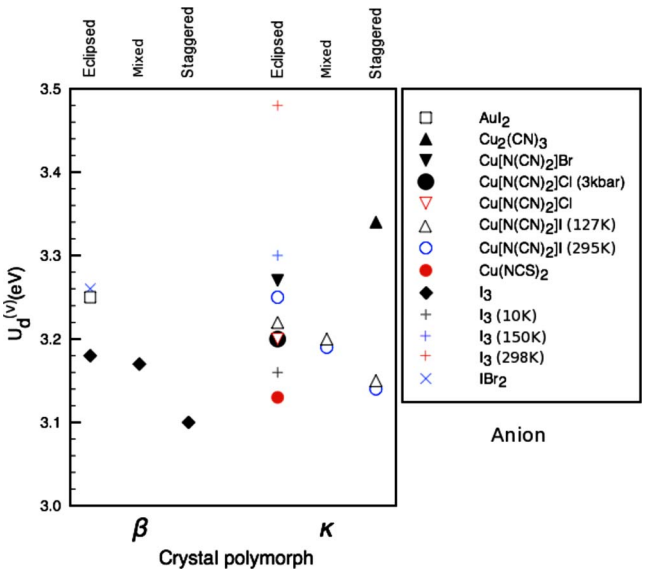

FIG. 7. (Color online) The effective intradimer Coulomb repulsion, $U_d^{(v)}$, for various ET dimers. The x axis separates the data by source crystal polymorph (β or κ) and by the terminal ethylene-group conformation of each ET molecule in the dimer. $U_d^{(v)}$ does not change significantly across the different ET crystals examined. For β-$(ET)_2X$ crystals, $U_d^{(v)} = 3.19 \pm 0.07$ eV. For κ-$(ET)_2X$ crystals, $U_d^{(v)} = 3.23 \pm 0.09$ eV. The difference in $U_d^{(v)}$ between the two crystal polymorphs is $\sim 1\%$. Therefore, there is no significant dependence of $U_d^{(v)}$ on the dimer geometry associated with different crystal polymorphs.

D. Variations in site energy and the role of disorder

As reviewed in Sec. I, a number of experiments have shown that disorder has strong effects on both the normal-state and superconducting properties of organic charge-transfer salts.[32,33,35–40] There has been relatively little work on the effect of the random-U Hubbard model. Conclusions drawn from studies in one dimension[56,57] cannot be straightforwardly generalized to higher dimensions. Mutou[58] used dynamical mean-field theory to study the metallic phase of the random-U Hubbard model. However, he did not consider the effect a random U on either superconductivity or the Mott transition, which are the primary concerns in the or-

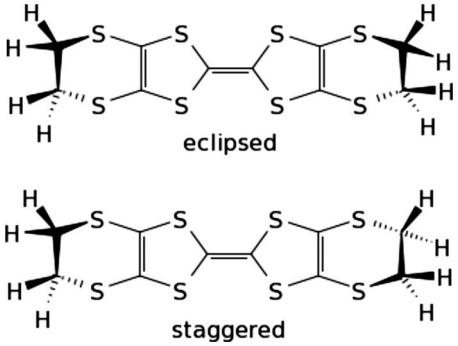

FIG. 8. ET molecules within the crystals studied occur in two conformations, denoted eclipsed and staggered. The difference between them lies in the relative orientation of the terminal ethylene groups.

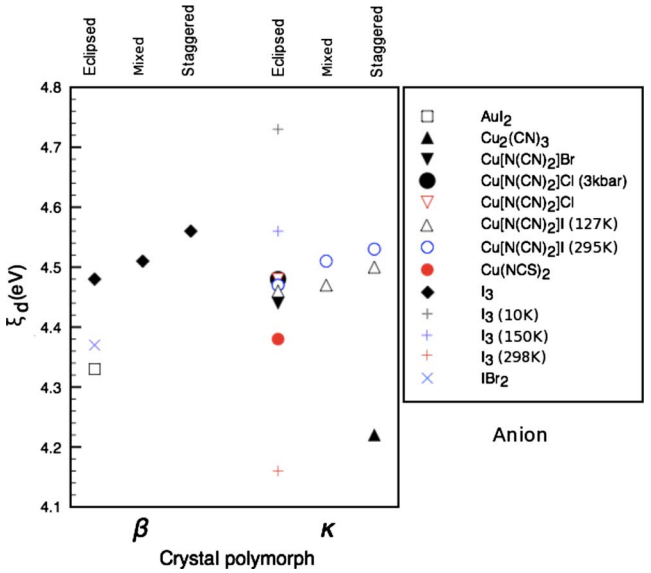

FIG. 9. (Color online) Dimer hole site energy, ξ_d, for various ET dimers. For β-$(ET)_2X$ crystals, the mean value is $\xi_d = 4.45 \pm 0.10$ eV. For κ-$(ET)_2X$ crystals, the mean value is $\xi_d = 4.46 \pm 0.14$ eV. The mean value for the whole data set is $\xi_d = 4.45 \pm 0.13$ eV. The effect of conformation on ξ_d is significantly larger for β-$(ET)_2I_3$ ($\sim 10\%$) than it is for the other parameters. The variations in ξ_d with dimer geometry associated with crystal polymorph and anion are $\sim 3\%$, similar to the relative variations in $U_d^{(v)}$ and $V_m^{(v)}$ across the whole data set.

ganic charge-transfer salts. However, Mutou concluded that for small impurity concentrations Kondo-type effects mean that the random-U Hubbard model is significantly different from the virtual-crystal approximation to the random-U Hubbard model, which describes the system in terms of an average U. The only study[59] we are aware of that discusses superconductivity in the random-U Hubbard model treats the negative U model, which is not realistic for the organic charge-transfer salts. Litak and Györffy[59] studied a model where some sites have $U=0$ and others have a negative U. They find that superconductivity is suppressed above at certain critical concentration of $U=0$ sites. Therefore, it is not clear what implications our finding of small changes in $U_d^{(v)}$ and hence U_d has for the physics of the organic charge-transfer salts. However, it is interesting to ask what role this plays in the observed role of disorder in suppressing superconductivity[32] and driving the system toward the Mott transition.[38] In this context it would be interesting to know whether the changes in the optical conductivity found by Sasaki *et al.*[60] in samples with disorder induced by x-ray irradiation can be explain in terms of a randomly varying U_d.

To understand the role of conformational disorder in terms of an effective Hamiltonian built up from ET dimers one must also understand the effect of conformational disorder of the effective dimer site energy (for holes), ξ_d. This is straightforwardly found from the DFT calculations described above via Eq. (3) and the results are reported in Fig. 9. The effective scattering rate due to conformational disorder is given by[61]

$$\frac{\hbar}{\tau} = \sum_i N_i \pi D(E_F) |\Delta_i \xi_d|^2, \tag{7}$$

where i labels the type of impurity (both staggered or mixed; the ground-state conformation is both eclipsed), N_i is number of impurities of type i, $D(E_F)$ is the density of states at the Fermi level, and $\Delta_i \xi_d$ is the difference between ξ_d for i-type impurities and ξ_d of eclipsed dimers.

In quasi-two-dimensional systems, $D(E_F)$ is simply related to the cyclotron electron mass[62] by the relation

$$D(E_F) = \frac{m_c}{2\pi\hbar^2} \tag{8}$$

and in the presence of interactions Luttinger's theorem[63] for a Fermi liquid produces

$$D(E_F) = \frac{m^*}{2\pi\hbar^2}, \tag{9}$$

where m^* is the effective mass. From quantum oscillation measurements, Wosnitza *et al.*[64] found that $m^*/m_e = 4.2$ in β-$(ET)_2I_3$, where m_e is the electron rest mass. From Shubnikov-de Haas measurements in κ-$(ET)_2Cu[N(CN)_2]Br$ Caulfield *et al.*[65] found that $m^*/m_e = 6.4$. The scattering rate τ can be found from measurement of the interlayer residual resistivity, ρ_0, by the relation[66]

$$\rho_0 = \frac{\pi\hbar^4}{2e^2 m^* c t_\perp^2 \tau}, \tag{10}$$

where c is the interlayer lattice constant taken from the relevant x-ray scattering measurements[48,51] and $t_\perp$ is the interlayer hopping integral, which has previously been estimated from experimental data for both κ-$(ET)_2Cu[N(CN)_2]Br$ (Ref. 64) and β-$(ET)_2I_3$ (Ref. 32). Using these parameters we calculated the scattering rate in both the β_L and β_H phases of β-$(ET)_2I_3$ from the low-temperature values of ρ_0 reported by Ginodman *et al.*[41] The scattering rate due to conformational impurities, τ_c^{-1} is then $\tau_c^{-1} = \tau_H^{-1} - \tau_L^{-1}$, where τ_L (τ_H) is the quasiparticle lifetime in the β_L (β_H) phase. Given our calculated values of $\Delta_i \xi_d$ an $\sim 8\%$ concentration of staggered impurities would be required to cause this scattering rate. From a similar calculation comparing the residual resistivity measured in a single sample of κ-$(ET)_2Cu[N(CN)_2]Br$ cooled at different rates we find that a $\sim 2\%$ concentration of staggered impurities would be sufficient to explain the rise increase in residual resistivity observed in the experiment utilizing the fastest cooling over that performed with the slowest cooling rate. X-ray scattering experiments[40] find that $3\% \pm 3\%$ of the ET molecules are in the staggered conformation at 9 K, which is entirely consistent with our result. However, Wolter *et al.*'s[40] argument that this impurity concentration is too small to cause the observed effects of disorder in not sustained by the above calculations. Rather we find that all of the suppression in T_c is entirely consistent with this degree of disorder.

E. Variations in intermonomer Coulomb repulsion

In Fig. 10 we show the distribution of the calculated values of $V_m^{(v)}$. The mean value of $V_m^{(v)}$ for the β-phase crystals is

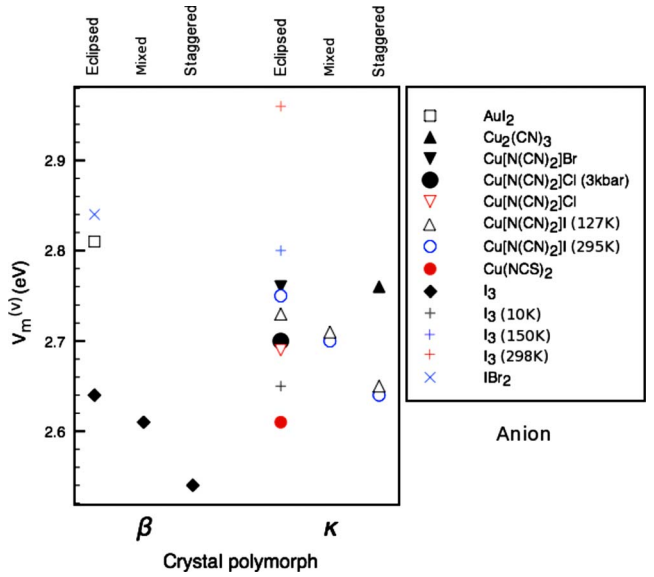

FIG. 10. (Color online) Intermonomer $V_m^{(v)}$ for various ET dimers. For β-$(ET)_2X$ crystals, $V_m^{(v)}=2.69\pm0.13$ eV and for κ-$(ET)_2X$ crystals, $V_m^{(v)}=2.72\pm0.09$ eV. The mean value is $V_m^{(v)}=2.71\pm0.10$ eV. The difference in $V_m^{(v)}$ between the crystal polymorphs is ~2%. Therefore, $V_m^{(v)}$, such as $U_d^{(v)}$, does not significantly depend on the geometry associated with crystal polymorph. The effect of ET conformation on the value of $V_m^{(v)}$ in the crystals β-$(ET)_2I_3$ and κ-$(ET)_2Cu[N(CN)_2]I$ is also similar to the effect on $U_d^{(v)}$. $V_m^{(v)}$ is lowest when the ET dimer has the staggered-staggered conformation and rises when either or both ET molecules are eclipsed.

2.69 ± 0.13 eV while the mean value for the κ-phase crystals is 2.72 ± 0.09 eV. Again, the difference between the values is small (~2%) as compared to the distribution for each polymorph. Therefore, $V_m^{(v)}$ is essentially the same across all of the conformations studied with a mean value of 2.71 ± 0.10 eV.

Previous calculations of $U_d^{(v)}$ based on both the Hückel method[24–31,55] and DFT (Refs. 14 and 15) have assumed that $U_m^{(v)}\to\infty$ and $V_m^{(v)}=0$. Substituting these conditions into Eqs. (2) and (5) yields $U_d^{(v)}=2t$. Literature values of $U_d^{(v)}$ based on this approximation are presented in Table I for comparison with our DFT results. It can be seen that this assumption yields values of $U_d^{(v)}$ that are significantly smaller than those we have calculated above (cf. Fig. 7). However, we have previously found[16] that $U_m^{(v)}=4.2\pm0.1$ eV. Comparing this with the above results we see that $U_m^{(v)}/V_m^{(v)}\sim1.5$, in contradiction of the assumption that $U_m^{(v)}\gg V_m^{(v)}$. Hence $U_m^{(v)}\gg|2t|$.

If we instead make the assumption $U_m^{(v)}\simeq V_m^{(v)}\gg|t|$, then Eqs. (2) and (5) give

$$U_d^{(v)}\approx\frac{1}{2}(U_m^{(v)}+V_m^{(v)}). \tag{11}$$

Substituting in the mean values of $U_m^{(v)}$ and $V_m^{(v)}$ gives $U_d^{(v)}=3.41$ eV. This result is close to (within 6% of) our calculated value of $U_d^{(v)}$. Therefore, this is a reasonable approximation for the ET salts. Further, this shows that the result that $U_d^{(v)}$ does not vary significantly because of changes in conformation between different salts or polymorphs is a consequence of the fact that neither $U_m^{(v)}$ nor $V_m^{(v)}$ vary significantly because of changes in conformation between different salts or polymorphs.

V. CONCLUSIONS

The effective Coulomb repulsion terms in the Hubbard model are essentially the same for all of the ET conformations studied. We found that $U_d^{(v)}=3.22\pm0.09$ eV and $V_m^{(v)}=2.71\pm0.10$ eV. The value of $U_d^{(v)}$ is significantly larger than previous estimates based on the extended Hückel formalism or DFT under the assumptions $U_m^{(v)}\to\infty$ and $V_m^{(v)}=0$. This can be understood because we have shown that $U_m^{(v)}\sim V_m^{(v)}$ and hence $U_d^{(v)}\approx\frac{1}{2}(U_m^{(v)}+V_m^{(v)})$.

The lack of variation in $U_d^{(v)}$ between the two polymorphs and when the anion is changed is interesting in the context of theories of these organic charge-transfer salts based on the Hubbard model. These theories require U_d/W to vary significantly as the anion is changed (chemical pressure) and under hydrostatic pressure. Therefore our results show that either $\delta U_d^{(p)}$ or W must vary significantly under chemical and hydrostatic pressures or else these theories do not provide a correct description of the β- and κ-phase organic charge-transfer salts. This is particularly interesting as fast cooling has been shown to drive κ-$(ET)_2Cu[N(CN)_2]Br$ to the insulating side of the metal-insulator transition.[38]

We have also studied the effects of conformational disorder on these parameters, which is found to be quite small, consistent with the often subtle effects of conformational disorder observed in these materials. The largest changes are found in the geometries taken from β-$(ET)_2I_3$, which shows the strongest effects of conformational disorder. It is also interesting that we found a systematic variation in $U_d^{(v)}$ is caused by conformational disorder. As there has been relatively little work on the random-U Hubbard model it is difficult to speculate what effects this has on the low-temperature physics of the organic charge-transfer salts at present.

Given that DFT band-structure parametrizations of the interdimer hopping integrals have recently been reported for several organic charge-transfer salts,[14,15] the outstanding challenge for the parametrization of the Hubbard model in these systems is the accurate calculation of $\delta U_d^{(p)}$. The bandwidth in both the β- (Ref. 13) and κ- (Refs. 14 and 15) phase salts is around 0.4–0.6 eV. Therefore, our finding that $U_d^{(v)}$ is significantly larger than has been realized previously shows that $\delta U_d^{(p)}$ must be significant as if $U_d\simeq U_d^{(v)}$ then all of these materials would be well into the Mott insulating regime. Thus $\delta U_d^{(p)}$ must significantly reduce U_d in order for the, observed, rich phase diagram to be realized. This is consistent with comparisons of dynamical mean-field theory (DMFT) calculations to optical conductivity measurements on κ-$(ET)_2Cu[N(CN)_2]Br_xCl_{1-x}$, which suggest that $U_d=0.3$ eV.[67] Further, $\delta U_d^{(p)}$ may be quite sensitive to the crystal lattice and therefore may be important for understanding the strong dependence of these materials on chemical and hydrostatic pressures.

ACKNOWLEDGMENTS

We thank Ross McKenzie for helpful comments on a draft of this manuscript. This work was supported by the Australian Research Council (ARC) under the Discovery scheme (Project No. DP0878523) and by a University of Queensland Early Career Research grant. B.J.P. was supported by the ARC under the Queen Elizabeth II scheme. Numerical calculations were performed on the APAC national facility under a grant from the merit allocation scheme.

*edan@physics.uq.edu.au

[1] G. R. Fleming and M. A. Ratner, Phys. Today **61** (7), 28 (2008).
[2] For a recent review, see A. J. Cohen, P. Mori-Sanchez, and W. T. Yang, Science **321**, 792 (2008).
[3] For a recent review, see G. Kotliar, S. Y. Savrasov, K. Haule, V. S. Oudovenko, O. Parcollet, and C. A. Marianetti, Rev. Mod. Phys. **78**, 865 (2006).
[4] B. J. Powell, *Computational Methods for Large Systems: Electronic Structure Approaches for Biotechnology and Nanotechnology*, edited by J. R. Reimers (Wiley, Hoboken, in press).
[5] For a recent review see B. J. Powell and R. H. McKenzie, J. Phys.: Condens. Matter **18**, R827 (2006).
[6] F. L. Pratt, S. J. Blundell, I. M. Marshall, T. Lancaster, C. A. Steer, S. L. Lee, A. Drew, U. Divakar, H. Matsui, and N. Toyota, Polyhedron **22**, 2307 (2003); F. L. Pratt and S. J. Blundell, Phys. Rev. Lett. **94**, 097006 (2005); B. J. Powell and R. H. McKenzie, J. Phys.: Condens. Matter **16**, L367 (2004).
[7] F. Kagawa, K. Miyagawa, and K. Kanoda, Nature (London) **436**, 534 (2005).
[8] Y. Shimizu, K. Miyagawa, K. Kanoda, M. Maesato, and G. Saito, Phys. Rev. Lett. **91**, 107001 (2003); P. A. Lee, Science **321**, 1306 (2008).
[9] A. C. Jacko, J. O. Fjærestad, and B. J. Powell, Nat. Phys. **5**, 422 (2009).
[10] J. Merino and R. H. McKenzie, Phys. Rev. B **61**, 7996 (2000); P. Limelette, P. Wzietek, S. Florens, A. Georges, T. A. Costi, C. Pasquier, D. Jerome, C. Meziere, and P. Batail, Phys. Rev. Lett. **91**, 016401 (2003).
[11] M. S. Nam, A. Ardavan, S. J. Blundell, and J. A. Schlueter, Nature (London) **449**, 584 (2007).
[12] B. J. Powell, E. Yusuf, and R. H. McKenzie, Phys. Rev. B **80**, 054505 (2009).
[13] Y. J. Lee, R. M. Nieminen, P. Ordejon and E. Canadell, Phys. Rev. B **67**, 180505(R) (2003).
[14] K. Nakamura, Y. Yoshimoto, T. Kasugi, R. Arita, and M. Imada, J. Phys. Soc. Jpn. **78**, 083710 (2009).
[15] H. C. Kandpal, I. Opahle, Y.-Z. Zhang, H. O. Jeschke, and R. Valentí, Phys. Rev. Lett. **103**, 067004 (2009).
[16] E. Scriven and B. J. Powell, J. Chem. Phys. **130**, 104508 (2009).
[17] R. L. Martin and J. P. Ritchie, Phys. Rev. B **48**, 4845 (1993).
[18] V. P. Antropov, O. Gunnarsson, and O. Jepsen, Phys. Rev. B **46**, 13647 (1992).
[19] M. R. Pederson and A. A. Quong, Phys. Rev. B **46**, 13584 (1992).
[20] G. Brocks, J. van den Brink, and A. F. Morpurgo, Phys. Rev. Lett. **93**, 146405 (2004).
[21] L. Cano-Cortés, A. Dolfen, J. Merino, J. Behler, B. Delley, K. Reuter, and E. Koch, Eur. Phys. J. B **56**, 173 (2007).
[22] See, for example, J. M., Williams, J. R. Ferraro, R. J. Thorn, K. D. Carlson, U. Geiser, H. H. Wang, A. M. Kini, and M.-H. Whangbo, *Organic Superconductors (Including Fullerenes): Synthesis, Structure, Properties and Theory* (Prentice Hall, New Jersey, 1992); E. Canadell, Chem. Mater. **10**, 2770 (1998); A. Painelli, A. Girlando, and A. Fortunelli, Phys. Rev. B **64**, 054509 (2001).
[23] H. Kino and H. Fukuyama, J. Phys. Soc. Jpn. **65**, 2158 (1996); R. H. McKenzie, Comments Condens. Matter Phys. **18**, 309 (1998).
[24] A. Kobayashi, R. Kato, H. Kobayashi, S. Moriyama, Y. Nishio, K. Kajita, and W. Sasaki, Chem. Lett. **16**, 459 (1987).
[25] M. Rahal, D. Chasseau, J. Gaulthier, L. Ducasse, M. Kurmoo, and P. Day, Acta Crystallogr., Sect. B: Struct. Sci. **53**, 159 (1997).
[26] T. Mori, Bull. Chem. Soc. Jpn. **71**, 2509 (1998).
[27] T. J. Emge. H. H. Wang, P. C. W. Leung, P. R. Rust, J. D. Cook, P. L. Jackson, K. D. Carlson, J. M. Williams, M.-H. Whangbo, E. L. Venturini, J. E. Schirber, L. J. Azevedo, and J. F. Ferraro, J. Am. Chem. Soc. **108**, 695 (1986).
[28] J. A. Schlueter, U. Geiser, H. H. Wang, A. M. Kini, B. H. Ward, J. P. Parakka, R. G. Daugherty, M. E. Kelly, P. G. Nixon, R. W. Winter, G. L. Gard, L. K. Montgomery, H.-J. Koo, and M.-H. Whangbo, J. Solid State Chem. **168**, 524 (2002).
[29] S. V. Simonov, I. Y. Shevyakova, L. V. Zorina, S. S. Khasanov, L. I. Buravov, V. A. Emel'yanov, E. Canadell, R. P. Shibaeva, and E. B. Yagubskii, J. Mater. Chem. **15**, 2476 (2005).
[30] A. Fortunelli and A. Painelli, J. Chem. Phys. **106**, 8051 (1997).
[31] C. E. Campos, P. S. Sandhu, J. S. Brooks, and T. Ziman, Phys. Rev. B **53**, 12725 (1996).
[32] B. J. Powell and R. H. McKenzie, Phys. Rev. B **69**, 024519 (2004).
[33] J. G. Analytis, A. Ardavan, S. J. Blundell, R. L. Owen, E. F. Garman, C. Jeynes, and B. J. Powell, Phys. Rev. Lett. **96**, 177002 (2006).
[34] M. V. Kartsovnik, P. D. Grigoriev, W. Biberacher, and N. D. Kushch, Phys. Rev. B **79**, 165120 (2009).
[35] X. Su, F. Zuo, J. A. Schlueter, A. M. Kini, and J. M. Williams, Phys. Rev. B **58**, R2944 (1998).
[36] X. Su, F. Zuo, J. A. Schlueter, M. E. Kelly, and J. M. Williams, Phys. Rev. B **57**, R14056 (1998).
[37] T. F. Stalcup, J. S. Brooks, and R. C. Haddon, Phys. Rev. B **60**, 9309 (1999).
[38] H. Taniguchi, K. Kanoda, and A. Kawamoto, Phys. Rev. B **67**, 014510 (2003).
[39] O. J. Taylor, A. Carrington, and J. A. Schlueter, Phys. Rev. B **77**, 060503(R) (2008).
[40] A. U. B. Wolter, R. Feyerherm, E. Dudzik, S. Süllow, Ch. Strack, M. Lang, and D. Schweitzer, Phys. Rev. B **75**, 104512 (2007).
[41] V. B. Ginodman, A. V. Gudenko, L. N. Zherikhina, V. N. Laukhin, E. B. Yagubskii, P. A. Kononovich, and I. F. Shegolev,

Acta Polym. **39**, 533 (1988).
[42] S. Ravy, J. P. Pouget, R. Moret, and C. Lenoir, Phys. Rev. B **37**, 5113 (1988).
[43] B. J. Powell, J. Phys. IV (France) **114**, 363 (2004).
[44] J. M. Soler, E. Artacho, J. D. Gale, A. García, J. Junquera, P. Ordejón, and D. Sánchez-Portal, J. Phys.: Condens. Matter **14**, 2745 (2002).
[45] J. P. Perdew, K. Burke, and M. Ernzerhof, Phys. Rev. Lett. **77**, 3865 (1996).
[46] O. F. Sankey and D. J. Niklewski, Phys. Rev. B **40**, 3979 (1989).
[47] N. Troullier and J. L. Martins, Phys. Rev. B **43**, 1993 (1991).
[48] P. C. W. Leung, T. J. Emge, M. A. Beno, H. H. Wang, J. M. Williams, V. Petricek, and P. Coppens, J. Am. Chem. Soc. **107**, 6184 (1985).
[49] H. H. Wang, M. A. Beno, U. Geiser, M. A. Firestone, K. S. Webb, L. Nuñez, G. W. Crabtree, K. D. Carlson, and J. M. Williams, Inorg. Chem. **24**, 2465 (1985).
[50] J. M. Williams, H. H. Wang, M. A. Beno, T. J. Emge, L. M. Sowa, P. T. Copps, F. Behroozi, L. N. Hall, K. D. Carlson, and G. W. Crabtree, Inorg. Chem. **23**, 3839 (1984).
[51] U. Geiser, A. J. Schultz, H. H. Wang, D. M. Watkins, D. L. Stupka, and J. M. Williams, Physica C **174**, 475 (1991).
[52] A. J. Schultz, U. Geiser, H. H. Wang, and J. M. Williams, Physica C **208**, 277 (1993).
[53] U. Geiser, H. H. Wang, K. D. Carlson, J. M. Williams, H. A. Charlier, Jr., J. E. Heindl, G. A. Yaconi, B. J. Love, and M. W. Lathrop, Inorg. Chem. **30**, 2586 (1991).
[54] V. Cocolicchio, J. Phys. A **33**, 5669 (2000).
[55] T. Komatsu, N. Matsukawa, T. Inoue, and G. Saito, J. Phys. Soc. Jpn. **65**, 1340 (1996).
[56] R. Ugajin, Phys. Rev. B **59**, 4952 (1999).
[57] A. W. Sandvik and D. J. Scalapino, Phys. Rev. B **47**, 10090 (1993).
[58] T. Mutou, Phys. Rev. B **60**, 2268 (1999).
[59] G. Litak and B. L. Györffy, Phys. Rev. B **62**, 6629 (2000).
[60] T. Sasaki, N. Yoneyama, Y. Nakamura, N. Kobayashi, Y. Ikemoto, T. Moriwaki, and H. Kimura, Phys. Rev. Lett. **101**, 206403 (2008).
[61] In the Born approximation the scattering rate for a random pattern of nonmagnetic impurities, represented by the potential $V(r)=\Sigma_i u_i \delta(\mathbf{R}_i-\mathbf{r})$, where $\mathbf{R}_i$ is the location of the ith impurity, is $\hbar/\tau=\Sigma_i N_i \pi D(E_F)|u_i|^2$ (Ref. 68). Equation (7) follows immediately as, for conformational impurities, $u_i=\Delta_i \xi_d$.
[62] J. Merino and R. H. McKenzie, Phys. Rev. B **62**, 2416 (2000).
[63] J. M. Luttinger, Phys. Rev. **121**, 1251 (1961).
[64] J. Wosnitza, G. Goll, D. Beckmann, S. Wanka, D. Schweitzer, and W. Strunz, J. Phys. I **6**, 1597 (1996).
[65] J. Caulfield, W. Lubczynski, F. L. Pratt, J. Singleton, D. Y. K. Ko, W. Hayes, M. Kurmoo, and P. Day, J. Phys.: Condens. Matter **6**, 2911 (1994).
[66] See, for example, R. H. McKenzie and P. Moses, Phys. Rev. Lett. **81**, 4492 (1998).
[67] J. Merino, M. Dumm, N. Drichko, M. Dressel, and R. H. McKenzie, Phys. Rev. Lett. **100**, 086404 (2008).
[68] G. Rickayzen, *Greens Functions and Condensed Matter* (Academic, London, 1980).